UNIVERSITY *of* York

This is a repository copy of *On Measurement of Reverberation Chamber Time Constant and Related Curve Fitting Techniques*.

White Rose Research Online URL for this paper:
https://eprints.whiterose.ac.uk/106189/

Version: Accepted Version

White Rose
university consortium
Universities of Leeds, Sheffield & York

eprints@whiterose.ac.uk
https://eprints.whiterose.ac.uk/

On Measurement of Reverberation Chamber Time Constant and Related Curve Fitting Techniques

X. Zhang, M. P. Robinson and Ian D. Flintoft

Department of Electronics, University of York, Heslington, York YO10 5DD, UK

On Measurement of Reverberation Chamber Time Constant and Related Curve Fitting Techniques

Xiaotian Zhang
Applied Electromagnetics Lab
Department of Electronics
Email: xz1148@york.ac.uk

Martin Robinson
Applied Electromagnetics Lab
Department of Electronics
Email: martin.robinson@york.ac.uk

Ian Flintoft
Applied Electromagnetics Lab
Department of Electronics
Email: ian.flintoft@york.ac.uk

Abstract—The reverberation chamber time constant quantifies how fast a reverberation chamber loses its stored energy at different frequencies, which makes it a very important parameter in many power related tests, such as the measurement of antenna efficiency, the measurement of absorption cross section, and the electromagnetic immunity test of electronic devices. The chamber time constant is usually obtained by doing regressions of power delay profile and calculating its gradient. But the shape of power delay profile can sometimes be distorted by the band limited window function applied in the frequency domain. A non-linear curve fitting technique which can cancel the effect of window function was developed, aiming to give a robust determination of the chamber time constant. With the help of this technique, window functions with much smaller bandwidth can be applied without introducing error in the evaluation of chamber time constant. In this paper, a 1 MHz wide window function in which only 10 samples of S_{21} are available was put under test and it was found a robust answer of chamber time constant can still be given by non-linear curve fitting techniques. Therefore the measurement time can be reduced and the frequency resolution of the chamber time constant can be increased at the same time.

Keywords: reverberation chamber, chamber time constant, power delay profile, non-linear curve fitting

I. INTRODUCTION

A reverberation chamber (RC) is a cavity loaded with a moving stirrer whose shape and size are carefully designed in order to create a stochastic field configuration. The applications of RC cover many areas ranging from communications to biomedical uses. Because it is a multipath environment in a RC, the RC can be used for simulating the indoor Rician channel with arbitrary K factor [1][2]. As a enclosed environment, it is relatively easy to build up a power balance model in an RC, thus making the RC very useful in a lot of power related tests such as the calibration of antenna efficiency [3], and determining the averaged absorption cross section(ACS) of a lossy object or human body [4][5].

The reverberation chamber time constant is a very important parameter, because it can give a lot of useful information about an operating RC, such as the total energy stored, rate of energy loss, total effective absorbing area [6] and so on. This information is very important to many electromagnetic compatibility (EMC) tests. For instance, the chamber time constant should be known before testing a pulse generator or a pulse radar, because a reverberation chamber with a high chamber time constant will change the pulse shape [7][8]. On the other hand, the total ACS of absorbers loaded in a reverberation chamber is found to be a function of chamber time constant, so the chamber time constant can tell the performance of absorbers [9].

The reverberation chamber time constant is usually obtained by doing linear regression of power delay profile (PDP) in the semi-logarithmic coordinate and calculating its gradient [11]. The PDP is the power response of a signal transmitted through a multipath channel as a function of time delay. A common way of getting PDP in a RC is to measure the frequency domain response and than calculate its inverse discrete Fourier transform (IDFT) within a small band. However, the PDP obtained in this way would have a "tail-like" form, where power rises rapidly at the end of the response, as can be easily seen in Fig.4 of [10], and Fig. 1 in this paper.

This "tail-like" form of PDP is caused by the ringing of band limited window function in time domain, which could not show the rate of power loss. Therefore the "tail" part should be gated away for doing linear regression when calculating the chamber time constant, but there are some problems with the gating techniques. Firstly, more data of PDP being gated away means less data remaining for doing linear curve fitting, thus lowering the accuracy of regression. Secondly, the position of gating is hard to choose because the boundary between the linear part and the non-linear "tail" is unclear. Including the "tail" into the linear regression would introduce error in the final results. Especially in broadband measurements, it is a great nuisance to check PDP frequency by frequency and choose a good linear curve fitting span.

This non-linear "tail-like" form is found to be caused by the band-limited window function applied in frequency domain (Details can be found in the followed Section II). So a non-linear curve fitting technique was developed which can fully cancel the effect coming from arbitrary window function. Because of the robustness of this new method, the window function with much smaller window width can be applied with no obvious change in the final output of chamber time constant. Thus the frequency resolution of chamber time constant can be increased at the same time.

II. THEORY

The mathematical definition of PDP is [3]

$$\text{PDP}(t_i) = <|h(t_i, n)|^2> \tag{1}$$

where $h(t_i, n)$ is the impulse response of a reverberation chamber, and because here it is a discrete series, t_i means

time with index i. The angle bracket "$< \cdot >$" means ensemble average over "n" independent stirrer positions.

Usually the impulse response $h(t_i, n)$ is obtained by doing IDFT of a frequency domain response (such as $S_{21}(f_k, n)$) filtered by a band-limited window function, as follows:

$$h(t_i, n) = \text{IDFT}\big[S_{21}(f_k, n) \cdot \text{win}(f_k)\big] \qquad (2)$$

where $\text{win}(f_k)$ is an arbitrary window function, f_k means frequency with index k in frequency domain. $h(t_i, n)$ would be changed by the application of different types of window functions.

To study the effect of window function on the PDP, one can start by generating $S_{21}(f_k, n)$ in an ideal reverberation chamber manually. The effect of the window function could then be predicted by filtering this S_{21} with specific window function.

The generation of S_{21} starts from the modeling of the ideal impulse response in time domain, and S_{21} can be obtained by just calculating the discrete Fourier transform (DFT). Three basic assumptions of an ideal reverberation chamber have been made and the ideas come from the "reverberation model" and "discrete multipath model" mentioned in Hill's review on the modeling of PDP in diffuse environment [11]:

1) Every single path in a reverberation chamber is fully band-pass, which means the shape of signal transmitted through any single path would not be distorted by losing part of its frequency components.

2) Because the power of received signal decays exponentially with time delay, so the mathematical model of ideal $S_{21}(f_k, n)$ should contain a exponential term like $e^{\frac{t_i}{\tau}}$, where τ is the chamber time constant, t_i is the time delay.

3) The reverberation chamber creates a multipath environment, therefore the signal received at any moment is the sum of signals transmitted through many independent paths. According to the central limit theorem, the total response of received signal at any moment would follow a Gaussian distribution.

In terms of all the three assumptions above, the original form of $S_{21}(f_k, n)$ is:

$$S_{21}(f_k, n) = \text{DFT}\big[h_{\text{ideal}}(t_i, n)\big] = \text{DFT}[Ae^{-\frac{t_i}{2\tau}} X_{0,1}(t_i)] \quad (3)$$

where $h_{\text{ideal}}(t_i)$ is the impulse response of an ideal reverberation chamber, which is not distorted by any window function; A is a constant which controls the amplitude of the response; there is a constant 2 in front of the chamber time constant τ because the loss of energy is two times slower than the drop of level of transmitted signal; $X_{0,1}(t_i)$ is a Gaussian random process with zero mean and unit variance. Because the variance of $h_{\text{ideal}}(t_i, n)$ at any moment can be controlled by A together with $X_{0,1}(t_i)$, the variance of $X_{0,1}(t_i)$ is set to be unit for easy application.

Eq.(3) can be substituted back to Eq.(2) to calculate the PDP. As an example, Fig 1 shows the generated PDP filtered
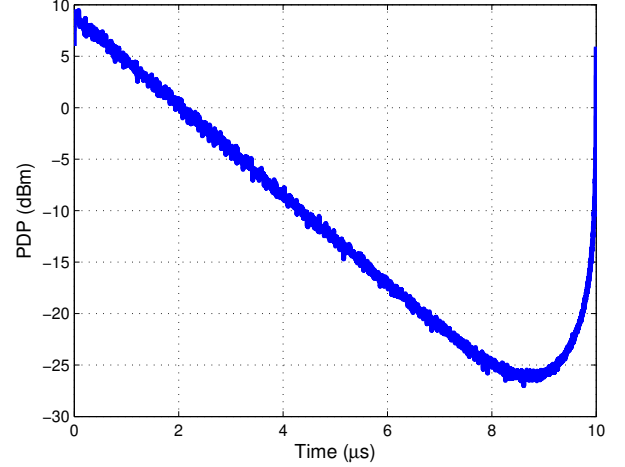

Fig. 1. The generated PDP filtered by 100 MHz rectangular window at 1 GHz

by a 100 MHz rectangular window at 1 GHz. The PDP is calculated by averaging over 200 independent sets of $h(t_i, n)$.

This model is not good for regression so far because it is a random process. What is needed is the expectation of Eq. 1 as the number of independent data sets tends to infinity.

Substituting Eq.(2) back into Eq.(1) and making use of the convolution theory, there is:

$$\text{PDP}(t) = < |Ae^{-\frac{t_i}{2\tau}} X_{0,1}(t_i)\text{Ⓝ}\text{IDFT}\big[\text{win}(f_k)\big]|^2 > \quad (4)$$

where "Ⓝ" means circulated convolution with resulting length N. The value of N is the number of full band responses of $S_{21}(f_k, n)$ which starts from zero frequency. In real measurements, if the measured $S_{21}(f_k, n)$ does not start from zero frequency, zero padding should be done from zero frequency to the minimum frequency of measured S_{21}. Also, The window function should also has the same vector length as the padded $S_{21}(f_k, n)$ does. Then taking advantage of the independent characteristic of Gaussian random process, the expectation of PDP can be calculated, and the form is simple:

$$\text{E}\big(\text{PDP}(t_i)\big) = A^2 e^{-\frac{t_i}{\tau}} \text{Ⓝ} \Big| \text{IDFT}[\text{win}(f_k)] \Big|^2 \quad (5)$$

The expectation of PDP is a circulated convolution of two power responses. This expectation can be used as a non-linear model for curve fitting because the random term $X_{0,1}(t_i)$ is gone, and the model is controlled by only two parameters - A and τ. The non-linear model can be imported into the MATLAB function "fit()" for the non-linear least square analysis, and the "Levenberg-Marquardt" algorithm is applied as a default algorithm of function "fit()" to search for the optimized value of A and τ [12]. But before doing the non-linear curve fitting, the starting values of A and τ should be set for the "Levenberg-Marquardt" algorithm.

Firstly, the starting value of τ can be simply selected as the output of linear regression of PDP. There is no need to worry about the selection of the curve fitting span in which

the shape of PDP is purely linear, because the output of linear regression is just used as a starting value, and the rest of the job of evaluating the chamber time constant is done by the "Levenberg-Marquardt" algorithm.

Secondly, the starting value of A is set to make the generated $S_{21}(f_k, n)$ have the same variance at a specific frequency as the measured $S_{21}(f_k, n)$ does, which is shown mathematically as follows:

$$\text{Var}\big[S_{21}(f_k = f_0, n)\big] = \text{Var}\big[S_{21,\text{meas}}(f_k = f_0, n)\big] \quad (6)$$

where $\text{Var}[\cdot]$ means to calculate the variance of S_{21} at a specific frequency over n different stirrer positions. f_0 is constant which shows where the frequency is. The subscript 'meas' at the right side of the equation means 'the measured data'.

Research found the variance of generated S_{21} in Eq.(6) has an analytic form. Here is a brief derivation. According to the convolution theorem, Eq.(3) changes into a form:

$$S_{21}(f_k, n) = \frac{1}{N}\text{DFT}(Ae^{-\frac{t_i}{2\tau}})\textcircled{N}\text{DFT}[X_{0,1}(t_i)] \quad (7)$$

The DFT of a Gaussian random process with unit variance would still be a Gaussian random process but with variance N which equals the number of responses. So Eq.(7) changes into:

$$S_{21}(f_k, n) = \frac{1}{N}\text{DFT}(Ae^{-\frac{t_i}{2\tau}})\textcircled{N}X_{0,N}(f_k) \quad (8)$$

Therefore the independent characteristic of Gaussian process can be used again here in calculating the variance of $S_{21}(f_k, n)$, the result is as follows:

$$\text{Var}[S_{21}(f_k = f_0, n)] = \frac{A^2}{N}\sum_{k=1}^{N}\big|\text{DFT}(e^{-\frac{t_i}{2\tau}})\big|^2 \quad (9)$$

Eq.(9) can be substituted back into Eq.(6) to calculate the starting value of A, which gives the form:

$$A = \sqrt{\frac{NS_{21,\text{meas}}(f_k = f_0, n)}{\sum_{k=1}^{N}\big|\text{DFT}(e^{-\frac{t_i}{2\tau}})\big|^2}} \quad (10)$$

Then the starting value of τ can be substituted into Eq.(10) to calculate the starting value of A.

III. Measurement

To validate the effectiveness of Eq.(5) in curve fitting, an experiment was done in the University of York reverberation chamber whose size is 4.70 m $\times$ 3.00 m $\times$ 2.37 m. The chamber was loaded with two horn antennas (ETS 3117 as transmitting antenna and ETS 3117 as receiving antenna). Both antennas were placed with boresights pointed away from each other in order to avoid direct coupling. There is a moving stirrer between two antennas which provided continuously changing boundary conditions. Both antennas are connected to a vector network analyzer Agilent E5071B via bulkheads
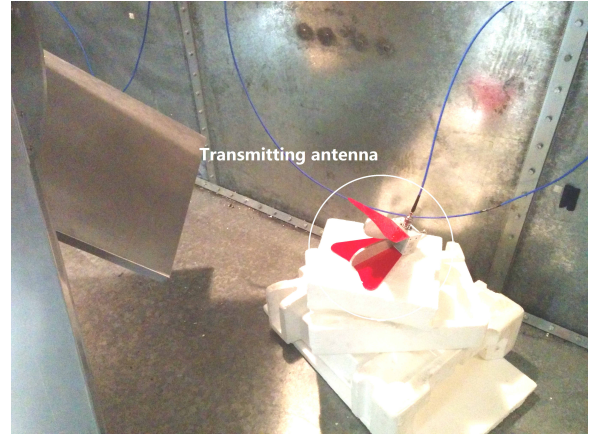

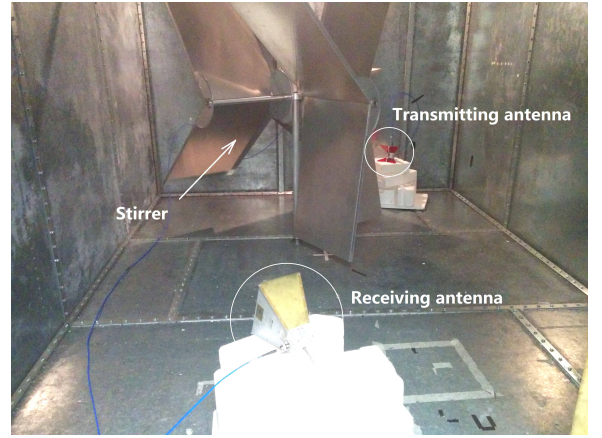Fig. 2.   Basic set up of experiment (transmitting antenna)

Fig. 3.   Basic set up of experiment (receiving antenna)

on the chamber wall. The diagram of experiment set up is shown in Fig. 2 and Fig. 3

The measurement ranges from 1 GHz to 7 GHz and the frequency step was set to be 100 kHz. The stirrer in the chamber was driven by a stepper motor which will move 200 steps so that 200 sets of independent sets of S_{21} can be measured. Firstly, a rectangular window whose width is 100 MHz was selected for validation, and the central frequency of the windows was randomly selected at 2 GHz, 4 GHz, 6 GHz. The PDP measured is as shown in Fig 4.

Even though the chamber time constant can be found by doing linear regression of PDP in Fig. 4, a good curve fitting span should be selected beforehand. Otherwise the non-linearity of filtered PDP would introduce error in the evaluation of chamber time constant. Fig. 5 shows the chamber time constant as a function of the linear curve fitting span, with the centre of the span fixed at 5 μs. Due to the shortage of data for linear curve fitting, the chamber time constant calculated firstly shows a big variation when the curve fitting span is smaller than 3 μs. Then the chamber time constant reaches a region where the curve is relatively flat, which means the linear curve fit gives a stable answer. But the chamber time constant rises as the curve fitting span keeps expanding, because the span starts to include some of the non-linear "tail" of the PDP in the linear regression. Because chamber time constant is a frequency-
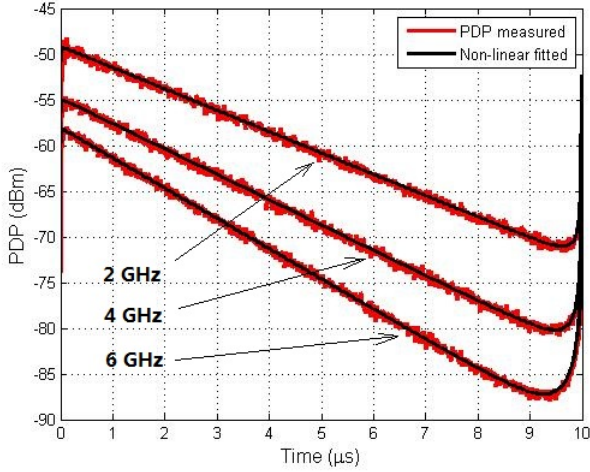
Fig. 4. Measured PDP (filtered by 100 MHz rectangular window) and non-linear curve fitting results
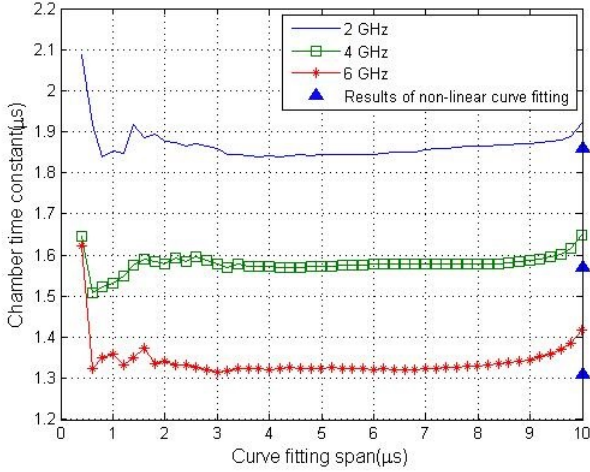

Fig. 5. Chamber time constant vs. linear curve fitting span (S_{21} filtered by an 100 MHz rectangular window)

dependent value, careful selection of curve fitting span should be done for each single frequency in wide band measurement. This is a very time consuming job if it is being done manually, and especially when the window width is small, it is more difficult to find a curve fitting span around which the output of chamber time constant is stable.

However, the whole range of PDP can be included in the non-linear curve fitting without introducing error because the non-linear curve fitting can fully describe the form of PDP in time domain. As shown in Fig. 4, the fitted curve matches well with the measured data from 0 μs to 10 μs. The chamber time constant given by non-linear curve fitting is also plotted as triangle marks in Fig. 5 for comparison. The results always locate at the flat region where the output of linear curve fitting converges, which shows the reliability of the non-linear curve fitting.

The chamber time constants obtained by non-linear regression are shown in Table. I and the coherence bandwidth is

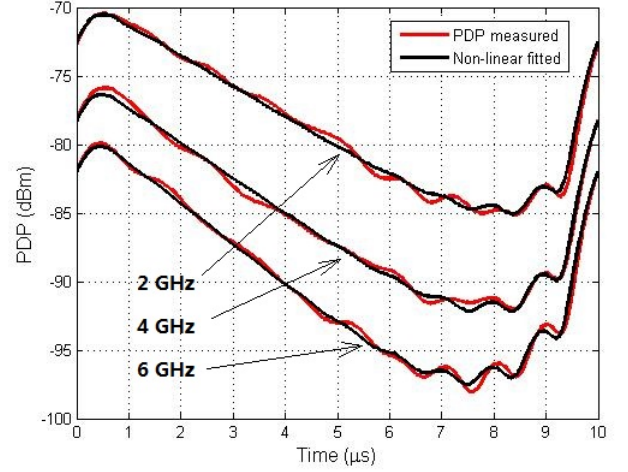| Frequency (GHz)	Chamber time constant (μs)	coherence bandwidth (MHz)
2	1.86	0.29
4	1.57	0.35
6	1.31	0.42

Fig. 6. Measured PDP (filtered by 1 MHz rectangular window) and non-linear curve fitting
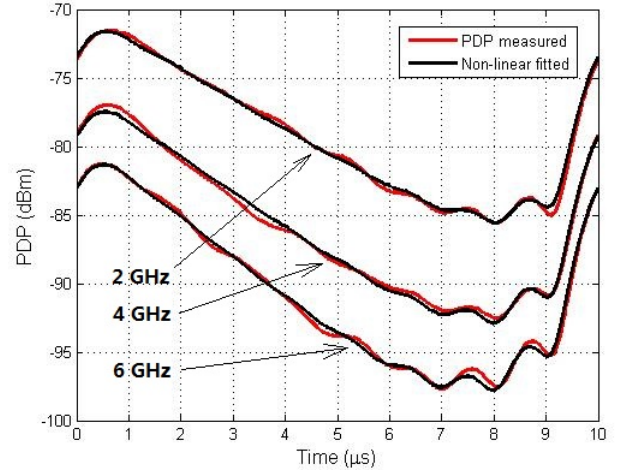

Fig. 7. Measured PDP (filtered by 1 MHz raised cosine window) and non-linear curve fitting

calculated as follows [13]:

$$\text{BW} = \frac{1}{\tau} \frac{\sqrt{3}}{\pi} \tag{11}$$

The coherence bandwidths are all smaller than 1 MHz, therefore the 100 MHz rectangular is too wide compared to the coherent bandwidth for doing inverse Fourier transform. A 1 MHz rectangular window was applied in obtaining the PDP, and the results are shown in Fig 6.

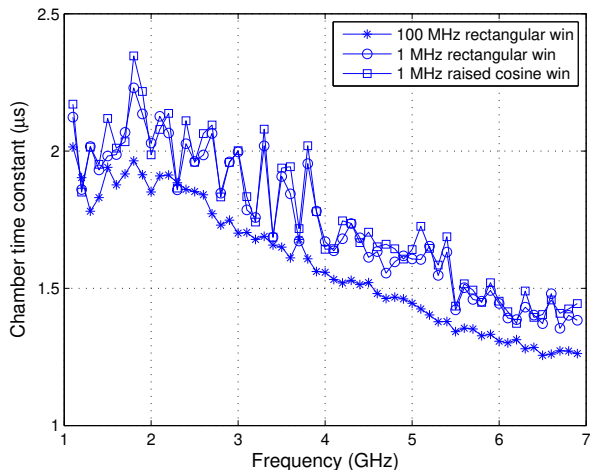When the window width is reduced to 1 MHz, the shape

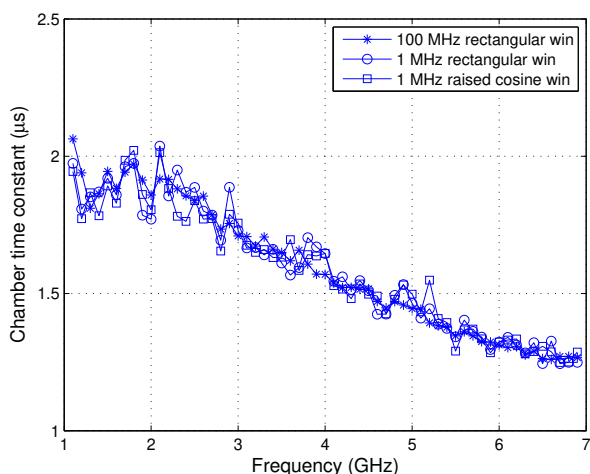Fig. 8.   Chamber time constant obtained by linear curve fitting

Fig. 9.   Chamber time constant obtained by non-linear curve fitting

of PDP is no longer suitable for linear curve fitting, while the non-linear curve fit can still do the job. Because the window function can be freely chosen, a raised cosine window[14] with 1 MHz total bandwidth and 0.25 rolling off factor has been tried. The results are shown in Fig. 7.

Fig. 6 and Fig. 7 clearly shows that the fitted curve matches well with the measurement data even though the width of window function is 1 MHz. Therefore the non-linear curve fitting could greatly increase the frequency resolution of chamber time constant.

Then the linear curve fitting and non-linear curve fitting was applied from 1 GHz to 7 GHz aiming to compare the robustness of two techniques. The chamber time constant obtained by the two different techniques was plotted in Fig. 8 and Fig. 9 The curve fitting span of linear curve fitting is selected to be from 1 μs to 4 μs over which the response of PDP is most likely to be linear.

The linear curve fitting is unstable. As the figures show, the chamber time constant obtained by linear curve fitting has

relatively bigger variation compared to that obtained by non-linear curve fitting. Also, the calculated chamber time constant changes as the width of window function is narrowed down from 100 MHz to 1 MHz.

However, the non-linear curve fitting is robuster. Although the different window functions were applied, the chamber time constants obtained are still quite close to each other. Especially, there are only 11 samples included for the calculation of PDP in a 1 MHz window, but the non-linear curve fitting could help giving a answer close to that when the 100 MHz window was applied. Therefore, with the help of non-linear curve fitting, only a few samples are needed around a fixed frequency point to get a reliable chamber time constant. This is very useful under the situations in which the measurement speed really matters, such as the measurement of absorption cross section of a human being who can not hold the same pose for a very long time.

IV.   CONCLUSION

A mathematical model of power delay profile in a reverberation chamber was firstly developed, which uses a robust non-linear curve-fitting method to calculate RC time constants. The non-linear curve-fitting model is controlled by just two different parameters, and it also takes the effect of the window function into account. This non-linear curve fitting has many advantages over linear curve fitting, in particular: 1. It can greatly increase the frequency resolution of chamber time constant calculations. 2. Only a few samples close to the central frequency need to be collected for obtaining these chamber time constants, so considerable measurement time can be saved. 3. The non-linear curve fitting takes all the data of the PDP into account, so it has the more efficient data usage, while the non-linear part of PDP would needed to be gated away for linear curve fitting. With the help of this non-linear curve fitting technique, the chamber time constant can be got much faster and more accurately, which accelerates many EMC tests, such as the measurement of antenna efficiency, the measurement of ACS, etc. Especially in the measurement of human body ACS, in which the human subject is not expected to hold the same pose for very long in the reverberation chamber, only a few frequency samples are needed to be collected for non-linear curve fitting, therefore the measurement can be finished quickly while the uncertainty coming from random body movement can be reduced at the same time.

REFERENCES

[1]   C. L. Holloway, D. A. Hill, J. M. Ladbury, P. F. Wilson, G. Koepke, and J. Coder, "On the use of reverberation chambers to simulate a rician radio environment for the testing of wireless devices," *Antennas and Propagation, IEEE Transactions on*, vol. 54, no. 11, pp. 3167–3177, 2006.

[2]   E. Genender, C. Holloway, K. Remley, J. Ladbury, G. Koepke, and H. Garbe, "Use of reverberation chamber to simulate the power delay profile of a wireless environment," in *Electromagnetic Compatibility-EMC Europe, 2008 International Symposium on*.   IEEE, 2008, pp. 1–6.

[3]   C. L. Holloway, H. A. Shah, R. J. Pirkl, W. F. Young, D. A. Hill, and J. Ladbury, "Reverberation chamber techniques for determining the radiation and total efficiency of antennas," *Antennas and Propagation, IEEE Transactions on*, vol. 60, no. 4, pp. 1758–1770, 2012.

[4] U. Carlberg, P.-S. Kildal, A. Wolfgang, O. Sotoudeh, and C. Orlenius, "Calculated and measured absorption cross sections of lossy objects in reverberation chamber," *Electromagnetic Compatibility, IEEE Transactions on*, vol. 46, no. 2, pp. 146–154, 2004.

[5] G. C. Melia, M. P. Robinson, I. D. Flintoft, A. C. Marvin, and J. F. Dawson, "Broadband measurement of absorption cross section of the human body in a reverberation chamber," *Electromagnetic Compatibility, IEEE Transactions on*, vol. 55, no. 6, pp. 1043–1050, 2013.

[6] J. B. Andersen, J. Nielsen, G. Pedersen, G. Bauch, and M. Herdin, "Room electromagnetics," *Antennas and Propagation Magazine, IEEE*, vol. 49, no. 2, pp. 27–33, 2007.

[7] T. Artz and H. Hirsch, "Pulsed signals in reverberation chambers: Modulating the input signal to reduce the rise-time," in *Electromagnetic Compatibility (EMC), 2013 IEEE International Symposium on*. IEEE, 2013, pp. 201–206.

[8] O. Lundén and M. Backstrom, "Absorber loading study in foi 36.7 m 3 mode stirred reverberation chamber for pulsed power measurements," in *Electromagnetic Compatibility, 2008. EMC 2008. IEEE International Symposium on*. IEEE, 2008, pp. 1–5.

[9] E. Amador, M. I. Andries, C. Lemoine, and P. Besnier, "Absorbing material characterization in a reverberation chamber," in *EMC Europe 2011 York*. IEEE, 2011, pp. 117–122.

[10] A. Bamba, W. Joseph, G. Vermeeren, E. Tanghe, D. P. Gaillot, J. B. Andersen, J. Ø. Nielsen, M. Lienard, and L. Martens, "Validation of experimental whole-body sar assessment method in a complex indoor environment," *Bioelectromagnetics*, vol. 34, no. 2, pp. 122–132, 2013.

[11] D. A. Hill, *Electromagnetic fields in cavities: deterministic and statistical theories*. John Wiley & Sons, 2009, vol. 35.

[12] W. H. Press, *Numerical recipes 3rd edition: The art of scientific computing*. Cambridge university press, 2007.

[13] C. L. Holloway, H. A. Shah, R. J. Pirkl, K. A. Remley, D. A. Hill, and J. Ladbury, "Early time behavior in reverberation chambers and its effect on the relationships between coherence bandwidth, chamber decay time, rms delay spread, and the chamber buildup time," *Electromagnetic Compatibility, IEEE Transactions on*, vol. 54, no. 4, pp. 714–725, 2012.

[14] I. Glover and P. M. Grant, *Digital communications*. Pearson Education, 2010.